

Nanosilicate Extraction from Rice Husk Ash as Green Corrosion Inhibitor

Denni Asra Awizar¹, Norinsan Kamil Othman^{1,*}, Azman Jalar², Abdul Razak Daud¹,
I. Abdul Rahman¹, N. H. Al-hardan²

¹School of Applied Physics, Faculty of Science and Technology,

²Institute of Micro Engineering and Nanoelectronics (IMEN); Universiti Kebangsaan Malaysia, 43600 UKM Bangi, Selangor Darul Ehsan, Malaysia

*E-mail: insan@ukm.my

Received: 1 October 2012 / Accepted: 7 January 2013 / Published: 1 February 2013

Silica was extracted from rice husk ash (RHA) and used to produce corrosion inhibitor for carbon steel. The particle size of the extracted silica was in the range 10-20 nm as measured using transmission electron microscopy (TEM). The corrosion inhibition efficiency of nanosilicate attained 99% as measured using the potentiodynamic polarization and weight loss measurements after 6 hrs exposures. It was found that the nanosilicate act excellently as corrosion inhibitor for carbon steel in distilled water medium. The surface morphology of carbon steel with and without inhibitor was investigated by SEM-EDX.

Keywords: Silicate; rice husk ash; corrosion; inhibition; polarization

1. INTRODUCTION

Corrosion is considered as one of the industrial problems, mainly in the systems involving water such as cooling systems and steel pipelines [1-2]. Furthermore it is one of the most important causes of destruction and loss of material. Corrosion also damages the operating equipment and hence demanding a high cost for maintenance [3]. Inhibitors are used to reduce the corrosion effect on the metal. The over use of inhibitors cause an additional problem such as environmental pollution [4]. The inorganic inhibitors were used in a very specific area due to their hazardous effect on human and the environment [5].

Recently, new generation of corrosion inhibitors were extracted from plants [6-12]. These natural corrosion inhibitors are inexpensive, available from renewable sources, easily produced and

considered as environmentally friendly compounds [13-15]. Furthermore, it solves the problem of using toxic compounds as corrosion inhibitors [16].

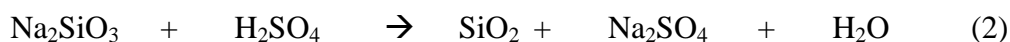
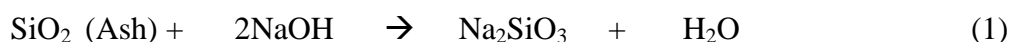
Silicate has been used as a corrosion inhibitor for years. It acts as anodic inhibitor, which adsorbs onto the metal surface to form a thin protective layer. Furthermore, silicate corrosion inhibitors are nontoxic and considered as natural corrosion inhibitor. [1, 4, 17-21].

In this paper silica was extracted from RHA. It is known that the silica content in RHA is more than 90% [22-25], which make it an economical extraction process. The extracted silica was used to produce a green corrosion inhibitor for carbon steel. It was tested in distilled water medium.

2. EXPERIMENTAL PART

2.1 Extraction of nanosilica

Silica was extracted using a method adapting from previous studies [22-25]. Paddy residue or rice husk was obtained from Kedah, a northern state of Malaysia. The rice husk was burnt to white ash. Subsequently silica was extracted from the white ash by 2.5M sodium hydroxide (NaOH) of solution, boiled for 3 hours, filtered, washed and dried at room temperature. A solution of 5M sulphuric acid (H₂SO₄) was added to produce silica with higher purity. Then it continued by refluxing process in acid condition (3M HCl) for 6 hours to obtained nanosilica powder. Followed by filtration and repeated washing. Solutions of 2.5M NaOH and 2.5M H₂SO₄ were added until pH neutral. The precipitating of nanosilica was washed and dried at 50 °C for 24 hours. The particle size of silica powder was determined by TEM (model Hitachi-700 at 100 kV). The extraction and purification occurred according to equations 1 and 2, respectively.



2.2 Inhibitor Solution

The nanosilicate solution inhibitor was prepared by dissolving 1 g of nanosilica powder in 3M NaOH solution. The pH value of the solution is 11.

2.3 Materials

Tests were performed on SAE 1045 carbon steel. The chemical composition of carbon steel is given in Table 1.

Table 1. Chemical composition of the SAE 1045 carbon steel (in wt%)

Elemental	C	Mn	P	S	Fe
Compositions	0.45	0.75	0.04	0.05	Bal.

2.4 Weight loss measurements

The carbon steel SAE 1045 rods were cut into pieces with a diameter of 15 mm in diameter and a thickness of 3 mm. The specimens were ground by a series of silicon carbide papers (grade 160-800), washed with distilled water, degreased with acetone and finally dried in flowing air. After weighing accurately by a digital balance, the specimens were immersed in distilled water in absence and presence of nanosilicate with different concentrations (5, 10, 15, 20 ppm). The experiment conducted at room temperature (25 °C) in the 6 days of immersion period. After immersion, the specimens were taken out, cleaned with bristle brush under running water in order to remove corrosion product, dried and reweighed accurately according to ASTM method [28]. Triplicate experiment was conducted. The differences in weights were noted and read averaged. Percentage of a inhibition efficiency (IE %) were calculated from corrosion rate data.

2.5 Potentiodynamic polarization measurements

Potentiodynamic polarization experiments were performed in a conventional three-electrode cell with a saturated calomel electrode (SCE) as the reference electrode, carbon counter electrode and working electrode (WE). The working surface area was 1.0 cm². The specimens were first immersed in the test solution for 30 min to attain a stable state. The polarization curves were acquired by scanning the potential from -0.25 to +0.25 mV with respect to free corrosion potential. Electrochemical measurements were carried out using a computer-controlled potentiostat (model K47 Gamry) at a scanning rate of 1.0 mV s⁻¹. Each experiment was repeated three times.

2.6 Surface morphological study

The surface morphology of the specimens after immersion into distilled water in the presence and absence of inhibitors was examined by scanning electron microscopy (SEM). The chemical composition of the film formed on the specimens surface was determined by energy dispersive x-ray analysis (EDX).

3. RESULTS AND DISCUSSION

3.1 Characteristic and morphology of nanosilica from RHA

The characteristics of the RHA content were identified before extraction of nano silica. The burning process of rice husk at 600°C for 6 hours produced rice husk ash which contained amorphous phase silica. Fig. 1 shows X-ray diffractograms of silica (SiO₂) of RHA. There are broad peaks at 23° theta. This broad peak confirmed the presence of amorphous phase silica [22-25]. The others X-rays diffractograms showed semicrystalline and crystalline phase of silica for combustion at 700°C and 900°C, respectively. Amorphous silica from RHA was important in this study, because it can be easily dissolved in certain media, it contains high porosity and high surface area [26-27].

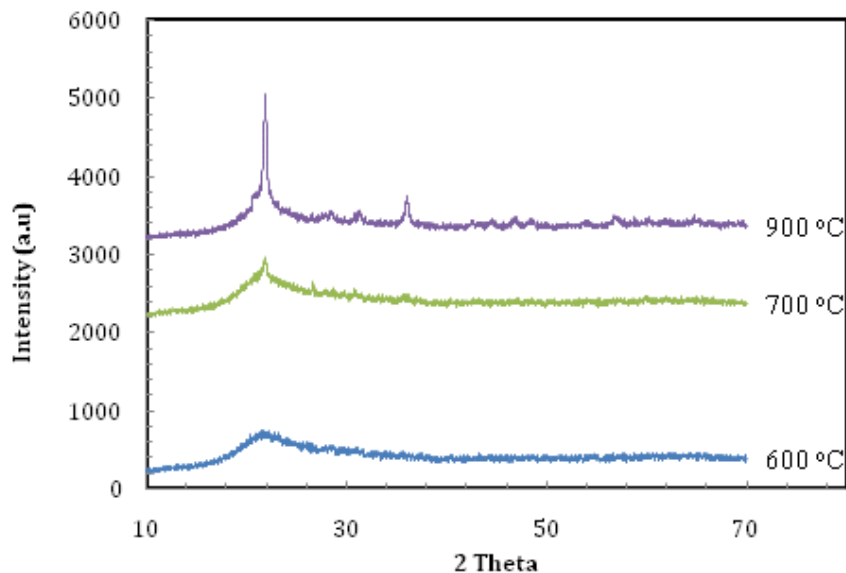


Figure 1. The X-ray diffractograms of RHA at different temperature burning

The elemental compositions of RHA were determined using XRF. The major elements were 51.23 of O and 42.44 of Si (% by weight). The remaining elements include metallic impurities such K, P, Mg, Ca, Fe, S, Na, Mn, Al, Zn, and Cl.

The morphology and particle size of nanosilica were examined by TEM. The particle size of nanosilica was obtained in nanometer scale in an agglomerated form. The particles were in spherical shape with diameter in the range of 5-20 nm, as can be seen in Fig. 2.

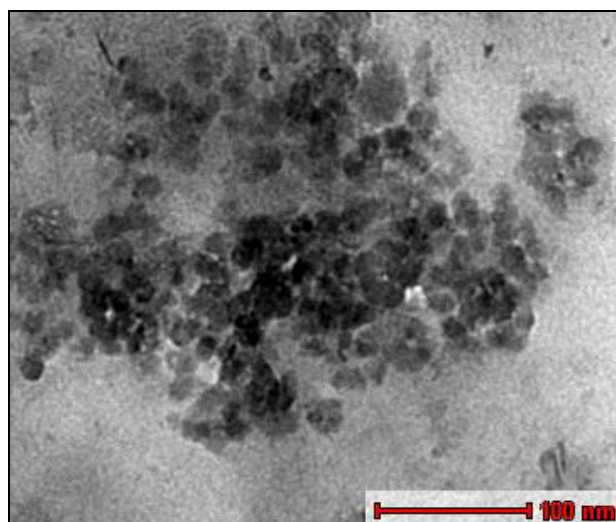


Figure 2. TEM micrographs of agglomerated nanosilica and the particles diameter is in the range of 5-20 nm

3.2 Weight loss measurements

The weight loss method is beneficial for monitoring inhibition efficiency due to its simple usage and reliability [10]. The effect of nanosilicate addition at different concentration on carbon steel in aqueous medium was studied by weight loss measurement at room temperature (25°C) or 6 days immersion period. The corrosion rate (CR) of carbon steel was calculated using equation 3.

$$CR(\text{mpy}) = \frac{534W}{DAT} \quad (3)$$

where W is weight loss in milligram, D density of sample (g/cm^3), A is area of sample in square inches, and T the exposure time in hours. From the value of weight loss in presence (W_1) and absence (W_0) of inhibitor, the inhibition efficiency (IE%) can be determined using the following equation 4.

$$IE \% = \left[1 - \frac{CR_1}{CR_0} \right] \times 100 \quad (4)$$

where (CR) refers to corrosion rate and the subscripts $_0$ and $_1$ refers to absence and presence of inhibitor in the solution respectively [8]. The results of the gravimetric determination of carbon steel in distilled water medium without and with addition of various concentrations of nanosilicate are summarized in Table 2. The CR of carbon steel decreased, whilst the percentage of inhibition efficiency increased when the concentration of inhibitors. Fig. 3 shows the change of IE (%) and CR with inhibitor concentrations. The inhibitor efficiency of nanosilicate attained increased from 85.3 to 99.5 (%) when the concentration of inhibitor was increased from 5 to 20 ppm. These results display the performance of nanosilicate from paddy residue as an excellent inhibitor. Even with small concentrations of inhibitor (ppm), satisfactory efficiency was obtained.

Table 2. Percentage inhibition efficiency (IE%) and corrosion rate (CR) at different concentrations of inhibitor in distilled water.

Inhibitor Concentration (ppm)	Weight loss (mg)	Corrosion Rate (mpy)	% Inhibition Efficiency
0	4.50	1.5386	-
5	0.70	0.2256	85.3 %
10	0.20	0.1368	91.1 %
15	0.10	0.0342	97.8 %
20	0.01	0.0084	99.5 %

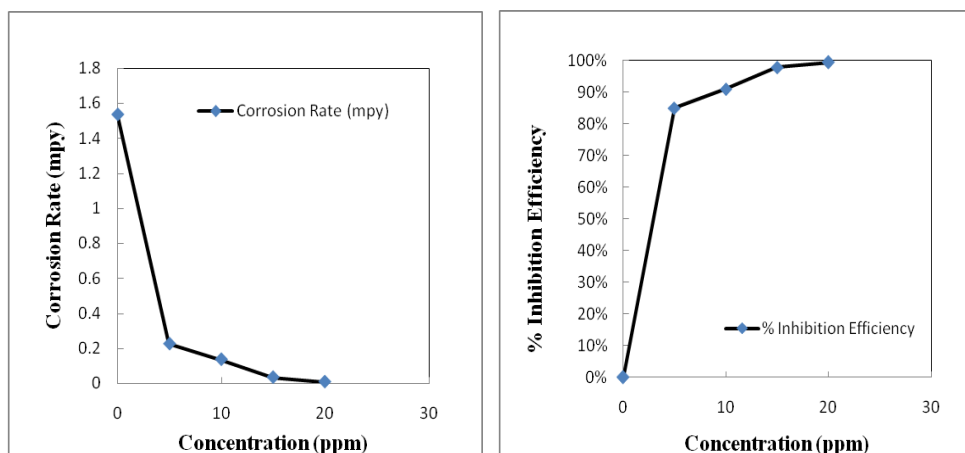


Figure 3. Corrosion rate and of inhibition efficiency with concentration of nanosilicate

3.3 Potentiodynamic measurements

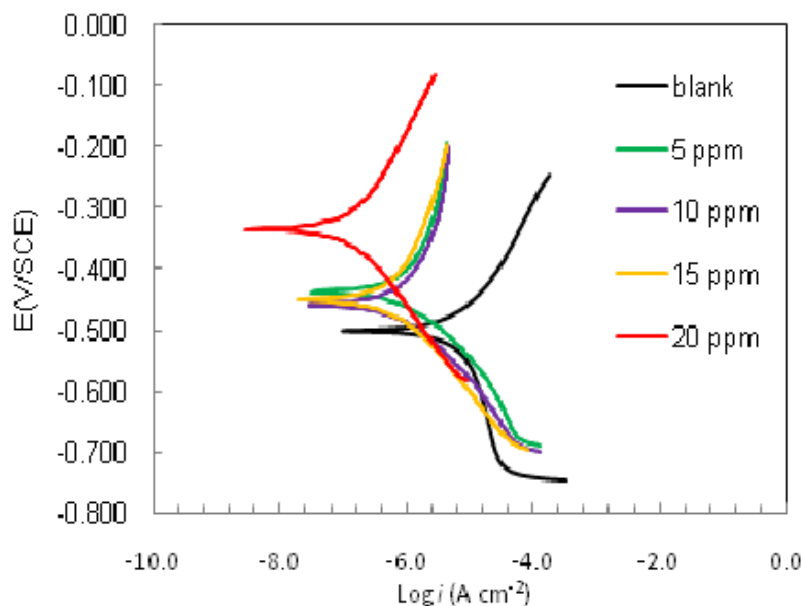


Figure 4. Potentiodynamic polarization curves for carbon steel in distilled water medium containing different concentrations of nanosilicate at room temperature (25°C).

Fig. 4 shows the anodic and cathodic polarization plots recorded for carbon steel in distilled water with the presence and absence of nanosilicate. Table 3 represents the electrochemical corrosion kinetic data, which include corrosion current density (I_{corr}), corrosion potential (E_{corr}), cathodic Tafel slope (b_c), anodic Tafel slope (b_a), and inhibition efficiency (IE). As it can be noticed, both anodic and cathodic reactions of the carbon steel corrosion electrodes were inhibited with the increase of nanosilicate concentration. This result suggests that the addition of nanosilicate inhibitors reduced the anodic dissolution and also retarded the cathodic reaction by blocking the steel surface from of oxygen [1, 29].

The corrosion potential (E_{corr}) showed a positive shift when treated with nanosilicate. The E_{corr}

changed from -499 to -334 (mV). This indicates that nanosilicate acts as anodic inhibitor for carbon steel. Additionally, table 3 exhibits that upon increasing the inhibitor concentration to 20 ppm, the corrosion current density decreased, whilst the inhibition efficiency increased tremendously. The highest *IE* (%) of 99 % occurred at 20 ppm of nanosilicate concentration. This is most likely due to the adsorption and formation of a good protective film by the nanosilicate inhibitor from the RHA.

The formation of a protective film is a result of the interaction of nanosilicate molecules with atoms of the base metal surface. The nano size silicate particles have high surface area that provides high reaction activities leading to increase in the formation of a protective film. Therefore, the surface of carbon steel has been block from is oxygen. This indicates that the inhibitor has provided a better protection at anodic sites.

Table 3. Potentiodynamic polarization data for corrosion of carbon steel in distilled water medium with different concentrations of nanosilicate.

Concentration (ppm)	I_{corr} (A cm^{-2})	E_{corr} (mVSCE)	b_c (mVdec^{-1})	b_a (mVdec^{-1})	R_p ($\text{k}\Omega\text{cm}^2$)	CR (mmpy)	IE (%)
0	14.76×10^{-6}	-499	628	237	5.067	0.117	-
5	1.943×10^{-6}	-437	155	700	28.40	0.023	86.8
10	1.401×10^{-6}	-459	140	421	32.51	0.016	90.5
15	0.856×10^{-6}	-450	139	344	48.81	0.010	94.2
20	0.170×10^{-7}	-334	155	206	227.2	0.002	98.8

Polarization Resistance (R_p) is related to the corrosion rate. A high R_p value reduces the corrosion rate. R_p value of lower than $20 \text{ k}\Omega \text{ cm}^2$ indicates an active corrosion condition, whereas R_p values greater than $100 \text{ k}\Omega$ indicates a passive condition [30]. The result in table 3 reveals that nanosilicate inhibitors have an average R_p value greater than $20 \text{ k}\Omega$. This indicates that nanosilicate effectively reduces corrosion. The R_p value was highest when the concentration of nanosilicate was 20 ppm. Resistance polarization and inhibition efficiency increased when inhibitor concentration was increased. The R_p value also indicated the formation of a thin film on the surface [1, 8, 11]. Furthermore, in the presence of the nanosilicate inhibitor, the cathodic Tafel slopes (b_c) were decreased significantly, while the anodic Tafel slopes (b_a) were decreased only at a higher inhibitor. This again indicates at nanosilicate is an anodic inhibitor which reduces anodic dissolution and consequently reduce on overall corrosion reaction [31, 32]. Fig. 5 depicts the proposed mechanism of the nanosilicate molecule adsorption. The negatively charged nanosilicate is attracted to the positively charged metal surface, which generates a bonding between the molecules and the surface. As a consequence, a protective layer is formed and corrosion attack is reduced.

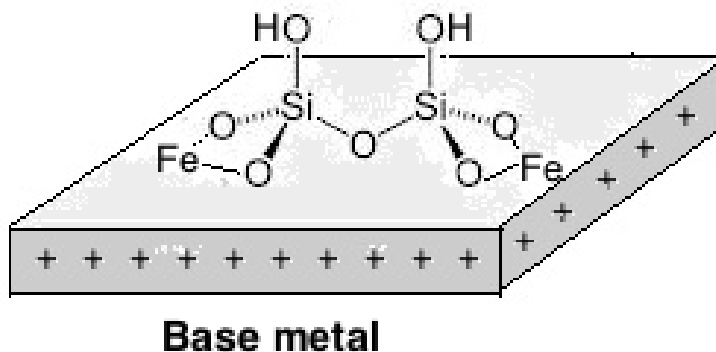
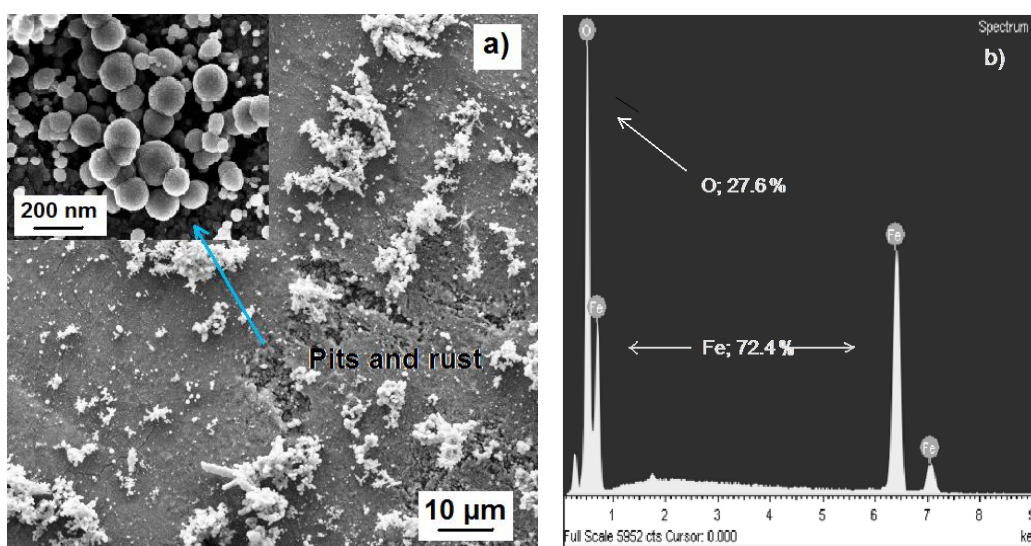


Figure 5. Schematic diagram of nanosilicate adsorption on the surface of carbon steel in distilled water

Salasi et al [1] reports that the inhibition behaviour of silicate inhibitor has a synergistic effect with the addition phosphonate in corrosion control of carbon steel in soft media. This result is still lower than the inhibition efficiency of nanosilicate extracted from rice husk ash, as highlighted in this study.

3.4 Surface morphology and component study

The efficiency in concentration inhibitor by nanosilicate is clearly visible in SEM images (Fig. 6). It shows the surface morphology of the carbon steel sample after 2 days immersion. Fig. 6(a) displays the SEM image of carbon steel surface after exposure in distilled water without inhibitors. The formation of rust and corroded surface is indicative of carbon steel unprotected condition of the carbon steel surface when nanosilicate was not present. Fig. 6(c) shows the surface morphology of the specimen after immersion in the distilled water containing 20 ppm of nanosilicate. Addition of nanosilicate resulted in the surface was free from corrosion. The surface seems compact and uniform.



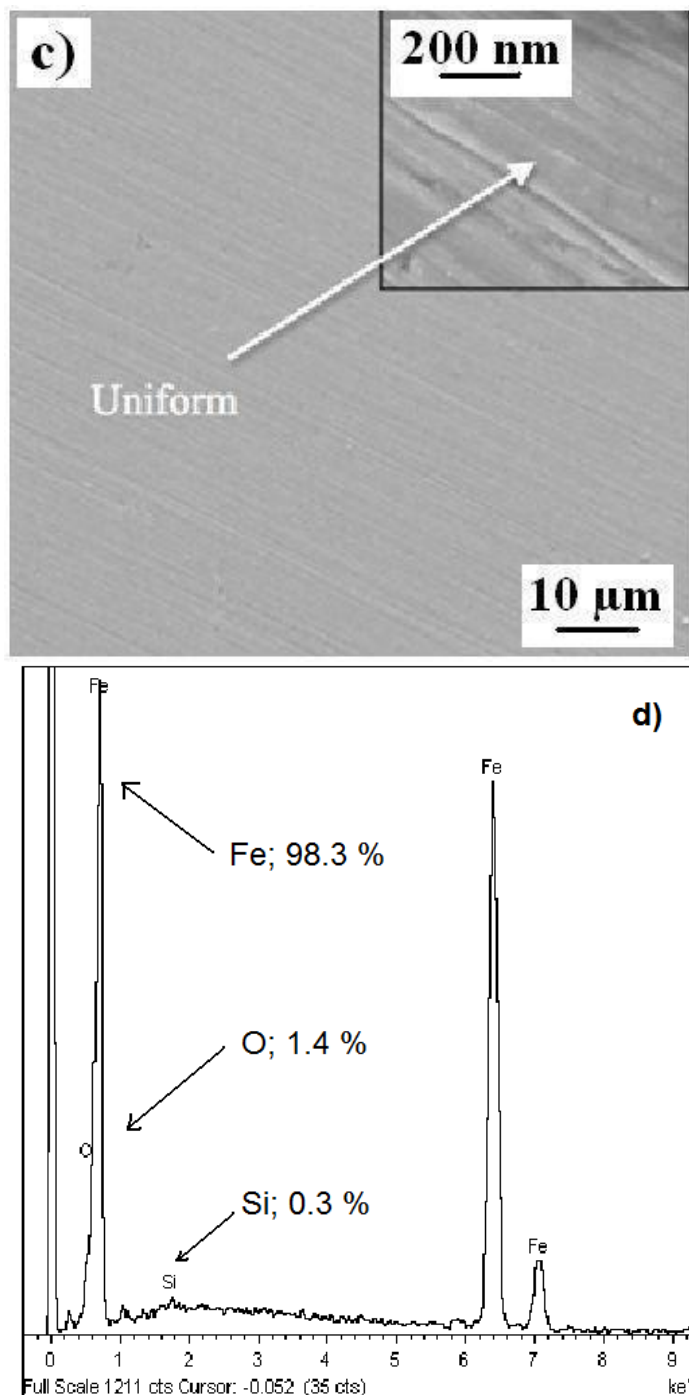


Figure 6. SEM images of specimen after immersion in distilled water medium, (a) absence and (c) presence inhibitors, whereas (b) and (d) are the EDX spectra for the corresponding SEM images in (a) and (c), respectively.

Fig. 6(b) and 6(d) show the EDX analyses on the surface of specimens in Fig. 6(a) and 6(c), respectively. Fig 6(b) reveals the EDX spectra of the surface in Fig 6 (a). It can be seen that the main elements in the surface are Fe and O. The element composition (in weight %) of Fe and O were 72.4 and 27.6, respectively. This indicates that the Fe has reacted with O from the medium (H_2O) to form iron oxide as a corrosion product. Fig. 6(d) shows the EDX spectrum of the surface in Fig. 6(c). The

percentage of Fe is 98.3% while O is 1.4%. This result exhibited low content oxygen. This small percentage of O may be contributed by the protective film of nanosilicate, which contained is 0.3% Si. The protective layer of nanosilicate inhibited the formation of iron oxide. Moreover, this experiment proved the excellent resistance of nanosilicate addition to carbon steel immersed in a distilled water medium.

3.5 Macrographic study

The macrographs of the specimens surface for 6 days immersion with the presence and absence of the nanosilicate corrosion inhibitor, is shown in Figs. 7 (a) to (d), with different of concentrations nanosilicate in the solution. The surface of steels exposed to inhibitor solution is brighter without visible corroded parts. The macrograph of carbon steel exposed in distilled water without nanosilicate clearly shows the present of rust (Fig. 7e). Therefore, it is proved that the nanosilicate is excellent corrosion inhibitor which provides stable protection to carbon steel from corrosion.



Figure 7. Macroscopical surface morphology of carbon steel samples after 6 days immersion in distilled water medium with the presence of (a) 5 ppm, (b) 10 ppm, (c) 15 ppm, (d) 20 ppm and (e) absence nanosilicate.

4. CONCLUSION

Natural nanosilica has been successfully extracted from rice husk and characterized by XRD and XRF. The nano-size of silica particles was confirmed by TEM. The inhibition efficiency of nanosilicate produced from nanosilica was determined by weight loss method and electrochemical polarization technique. The inhibition efficiency attained was about 99 % at 20 ppm of nanosilicate was added into distilled water medium. The corrosion rate of carbon steel significantly decreased with the presence of inhibitor. Polarization test revealed that the nanosilicate is an anodic inhibitor. The introduction of nanosilicate into distilled water medium resulted in the formation of a thin protective film on the carbon steel surface. The particle size plays an important role in retarding corrosion. The silicate nanosize has a high surface area that provides higher reaction activities, effectively increasing the formation of the protective film. It effectively protects the carbon steel surface from corrosion. Nanosilicate produced from RHA shows an excellent corrosion inhibitor for carbon steel.

ACKNOWLEDGEMENT

The authors would like to thank all the colleagues from School of Applied Science and Faculty of Science of Engineering UKM for their assistance throughout this study, particularly to staff of MIPAC

and IMEN UKM. The authors also gratefully to the Government of Malaysia and UKM for financial support through several funds (UKM-GGPM-089-2010, 03-01-02-SF0734, DIP-2012-14 and ERGS/1/2012/STG05/ukm/02/2).

References

1. M. Salasia, T. Shahrabia, E. Roayaeib, M. Aliofkhazraeia, *Mater. Chem. and Phys.*, 104 (2007) 183
2. D. Konstantinos, Demadis, E. Mavredaki, A. Stathouloupoulou, E. Neofotistou, C. Mantzaridis, *Desalination*, 213 (2007) 38
3. V. S. Sastri, E. Ghali and M. Elboujdaini, Editor, Corrosion Prevention and Protection Practical Solutions. John Wiley & Sons. Publishers, Ottawa (2007)
4. H. Gao, Q. Li, F. N. Chen, Y. Dai, F. Luo, L.Q. Li, *Corros. Sci.*, 53 (2011) 1401
5. E. W. Flick, Corrosion Inhibitors-An Industrial Guide. Noyes Publication, USA (1993).
6. O. K. Abiola, J.O.E. Otaigbe, O. J. Kio, *Corros. Sci.*, 51 (2009) 1879
7. P. B. Raja, M. G. Sethuraman, *Materials* 62 (2008) 113
8. M. Belloa, N. Ochoaa, V. Balsamoa, F. L. Carrasquerob, S. Collc, A. Monsalved, G. Gonzálezd , *Carbohydrate Polymers* 82 (2010) 561
9. J.C.Da Rocha, J. A.da Cunha Ponciano Gomes, E.D'Elia, *Corros. Sci.* 52 (2010) 2341
10. N. O. Obi-Egbedi, I.B. Obot, S. A. Umoren, *Arab. J. Chem.*, 5 (2012)5, 361
11. A. Lecante, F. Robert, P. A. Blandinières, C. Roos, *Curr. Appl Phys.* 11 (2011) 714
12. O. K. Abiola, A.O. James, *Corros. Sci.* 52 (2010) 661
13. A. Ostovari, S.M. Hoseinie, M. Peikari, S.R. Shadizadeh, S.J. Hashemi, *Corros. Sci.*, 51 (2009) 1935
14. S. Deng, X. Li, *Corros. Sci.*, 55 (2012) 407
15. O. K. Abiola, J.O.E. Otaigbe, *Corros. Sci.* 51 (2009) 2790
16. I. Radojic, K. Berkovic, S. Kovac, J. V. Furac, *Corros. Sci.*, 50 (2008) 1498
17. K. Aramaki, *Corros. Sci.*, 43 (2001) 591
18. Y. Xu, B. Lin, *Trans. Nonferrous Met. Soc. China*, 17 (2007) 1248
19. S. T. Amaral, I.L. Müller, *Corros. Sci.* 41 (1999) 747
20. J. C. Rushing, L.S. McNeill, M. Edwards, *Water Res.*, 37 (2003) 1080
21. B. Lin, J. Lu, G. Kong, *Surf. Coat. Technol.*, 202 (2008) 1831
22. Y. Yaacob, S. Z. Saad, M. R. Othman, N. H. Mohd Noor, *Int. J. Nanotech. Applic.*, 4 (2010) 61
23. C. Real, M. Alcala, J.M. Criado, *J. Am. Ceram Soc.*, 79 (1996) 2012
24. K. Amutha, R. Ravibaskar and G. Sivakumar, *Int. J. Nanotech. Applic.*, 1 (2010) 61
25. N. Thuadaj and A. Nuntiya, *Chiang Mai J. Sci.*, 35 (2010) 206
26. S. H. Javed, S. Tajwar, M. Shafaq, M. Zafar, M. Kazmi, *J. Pakistan Inst. Chem. Eng.*, 37 (2008)
27. V. P. Della, I. Kuhn, D. Hotz, *Mater. Lett.* 57 (2002) 818
28. S. Deng, X. Li, *Corros. Sci.*, 55 (2012) 407–415
29. M. G. Fontana, Corrosion engineering third edition, McGraw-hill book co-Singapore, (1986).
30. A. E. Martell, M. Calvin, *J Electrochem Soc.*, 104 (1957) 56
31. D. A. Jones, Principle and Prevention of Corrosion 2nd edition, Prentice Hall, NT USA (1996)
32. A. Phanasgaonkar, V. S. Raja, *Surf. & Coatings Tech.*, 203 (2009) 2260